Fine-tuning the release of molecular guests from mesoporous silicas by controlling the orientation and mobility of surface phenyl substituents

*J. Sebastián Manzano,[†] Dilini Singappuli-Arachchige,[†] Bosky L. Parikh, Igor I. Slowing**

US DOE Ames Laboratory, Ames, IA 50011, United States

Department of Chemistry, Iowa State University, Ames, IA 50011, United States

[†]These authors contributed equally to this study.

*Corresponding author, E-mail address: islowing@iastate.edu

Abstract

Phenyl-functionalized mesoporous silica materials were used to explore the effect of non-covalent interactions on the release of Ibuprofen into simulated body fluid. Variations in orientation and conformational mobility of the surface phenyl groups were introduced by selecting different structural precursors: 1) a rigid upright orientation was obtained using phenyl groups directly bound to surface Si atoms (Ph-MSN), 2) mobile groups were produced by using ethylene linkers to connect phenyl groups to the surface (PhEt-MSN), and 3) groups co-planar to the surface were obtained synthesizing a phenylene-bridged periodic mesoporous organosilica (Ph-PMO). The Ibuprofen release profiles from these materials and non-functionalized mesoporous silica nanoparticles (MSN) were analyzed using an adsorption-diffusion model. The model provided kinetic and thermodynamic parameters that evidenced fundamental differences in drug-surface interactions between the materials. All phenyl-bearing materials show lower Ibuprofen initial release rates than bare MSN. The conformationally locked Ph-MSN and Ph-PMO have stronger interactions with the drug (negative ΔG of adsorption) than the flexible PhEt-MSN and bare MSN (positive ΔG of adsorption). These differences in strength of adsorption are consistent with differences between interaction geometries obtained from DFT calculations. B3LYP-D3-optimized models show that π-π interactions contribute more to drug adsorption than H-bonding with silanol groups. The results suggest that the type and geometry of interactions control the kinetics and extent of drug release, and should therefore serve as a guide to design new drug delivery systems with precise release behaviors customized to any desired target.

Keywords

Drug delivery systems, Mesoporous Silica Nanoparticles, Controlled release, Interface, Polarity, Ibuprofen

1. Introduction

Advancements in drug delivery systems (DDS) are of utmost importance to the development of the pharmaceutical and biomedical fields. One of the key properties of advanced DDS is the ability of releasing drug molecules in a controlled fashion. In this respect, mesoporous silicas have been extensively studied as promising DDS because in addition to their biocompatibility, controllable pore structure, large pore volumes and surface areas, they can be functionalized with a wide variety of moieties.[1-5] These properties have enabled the design of gated DDS that release their cargo upon application of specific stimuli like radiation, changes in pH, temperature, redox potentials, magnetic fields, or signaling molecules.[6-12] Furthermore, these materials have also been modified with receptors, antibodies, or aptamers to provide targeting capabilities, and with reactive moieties to control cell internalization and endo/lysosomal escape.[13-18]

In spite of all these sophisticated designs and their successful *in vitro* and *in vivo* applications,[19-21] little attention has been paid to the influence of drug-surface interactions on the extent and kinetics of release. Moreover, our understanding of the role of organic moieties on surface-solvent partition equilibria and diffusion rates of the loaded drugs is fairly limited and often overlooked. This is surprising given the importance usually attributed to the high surface area and the ability to tailor the surface chemistry of these materials. Initial efforts to determine the effects of surface groups on

the performance of mesoporous silica DDS were conducted by Vallet-Regí and co-workers when studying Erythromycin release as a function of alkyl substitution.[22] Their results showed that release was affected by surface hydrophobicity, and suggested that partition equilibria between the surface and the media controlled drug discharge. More recently, Berger and collaborators investigated the effects of group functionalities on the release of Metoprolol from mesoporous silica.[23] They observed a correlation between functional group pK_a and the amount of drug released, suggesting that electrostatic interactions controlled release rates. Interestingly, computational studies by Ugliengo and co-workers suggested that even weak interactions can determine drug release. Their simulations showed that London dispersion forces play a more important role than H-bonding in the adsorption of Ibuprofen on the silica surface.[24, 25] However, NMR and relaxation dielectric spectroscopy studies have shown that the interaction of Ibuprofen with the silica surface is so weak that only a fraction of the drug is adsorbed to the pore walls and the rest exists as highly mobile species.[26-31] Thus, one can expect that producing gradual enhancements of the drug-silica interactions may allow fine-tuning drug release.

Herein, with the aim of enabling precise control of drug release rates, we explore the potential role of non-covalent interactions on the behavior of mesoporous silica-based DDS. Specifically, we investigate the effect of π-π interactions between Ibuprofen and surface-immobilized phenyl groups on its release kinetics from silica carriers. To this end, we produced phenyl-functionalized mesoporous silicas with different structural features, namely: 1) mesoporous silica nanoparticles (MSN) with phenyl groups directly bound to silicon atoms (Ph-MSN) where groups are rigid and upright, 2) MSN with

phenyl groups attached via flexible ethylene linkers (PhEt-MSN) where groups have conformational mobility, and 3) phenylene-bridged periodic mesoporous organosilica (Ph-PMO) where the phenyl group is co-planar to the pore surface (Scheme 1). We compared the Ibuprofen release profiles from these materials and non-functionalized MSN to assess the effects of orientation (perpendicular versus co-planar to the pore walls) and conformational flexibility on the strength of interactions and release kinetics of the drug. By fitting the release profiles to a three-parameter kinetic model developed by Zeng and Wu, we characterized the thermodynamics of surface-solvent partition and the diffusion kinetics of the desorbed molecules from the pores to the bulk media.[32, 33] Finally, we pursued an atomistic level understanding of the interactions via computational modeling of drug-surface complexes using a silica surface model developed by Ugliengo and co-workers.[34, 35]

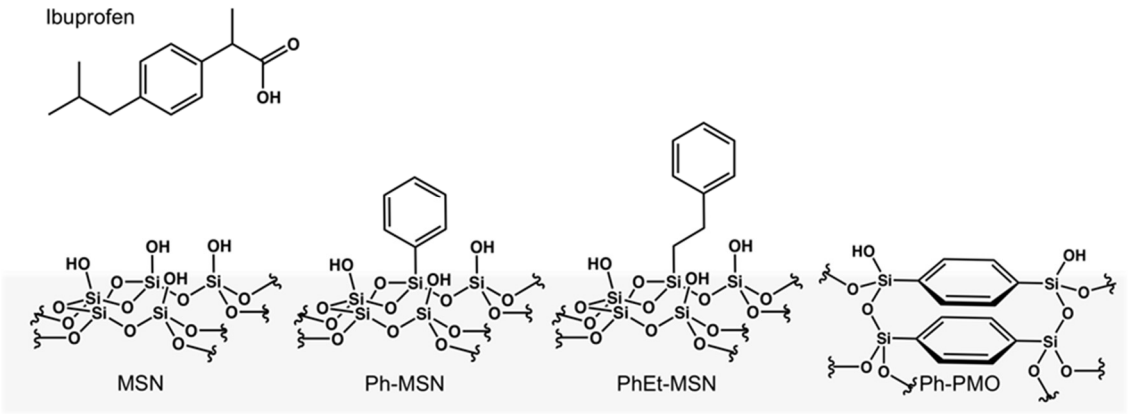

Scheme 1. Structure of Ibuprofen and surface functionalities of the four mesoporous silica based DDS.

2. Methods

2.1 Chemicals

Hexadecyltrimethylammonium bromide (CTAB), Brij 76 ($C_{18}EO_{10}$) and Ibuprofen were purchased from Aldrich. Tetraethylorthosilicate (TEOS), phenyltrimethoxysilane, phenethyltrimethoxysilane and 1,4-bis(triethoxysilyl) benzene were purchased from Gelest, Inc. NaOH, NaCl, KCl, K_2HPO_4, $MgCl_2 \cdot 6H_2O$, $CaCl_2$, Na_2SO_4, Tris(hydroxymethyl)aminomethane, conc. HCl and acetone were purchased from Fisher Scientific. $NaHCO_3$ was from Alfa Aesar, and Prodan from Anapec, Inc. All chemicals were used as received without any further purification.

2.2 Synthesis of MSN

CTAB (1.0 g, 2.74 mmol) was dissolved in deionized water (480 ml) in a round bottom flask followed by addition of 2 M NaOH (3.5 mL, 7.0 mmol). The solution was stirred for 1 h at 80 °C. TEOS (5.0 mL, 22.6 mmol) was then added drop wise over 5 min to the CTAB solution. Magnetic stirring was continued for another 2 h at 80 °C. The solution was filtered, washed with abundant water and methanol, and vacuum dried overnight. CTAB was removed by refluxing 1.0 g of dry solid with 100 mL of methanol and conc. HCl (0.8 mL, 9.7 mmol) at 60 °C for 6 h. The surfactant removal step was repeated. The surfactant-removed sample was then filtered, washed with abundant methanol and vacuum dried overnight.

2.3 Synthesis of Ph-MSN and PhEt-MSN

CTAB (1.0 g, 2.74 mmol) was dissolved in deionized water (480 ml) in a round bottom flask followed by addition of 2 M NaOH (3.5 mL, 7.0 mmol). The solution was stirred for 1 h at 80 °C. TEOS (5.0 mL, 22.6 mmol) and phenyltrimethoxysilane (0.19 mL, 1.0 mmol) for Ph-MSN or phenethyltrimethoxysilane (0.22 mL, 1.0 mmol) for PhEt-MSN were then added drop wise over 7 min to the CTAB solution. Magnetic stirring was continued for another 2 h at 80 °C. The solution was filtered, washed with abundant water and methanol respectively, and vacuum dried overnight. CTAB template was removed by refluxing 1.0 g of dry solid with 100 mL of methanol and conc. HCl (0.8 mL, 9.7 mmol) at 60 °C for 6 h. The surfactant removal step was repeated. The surfactant-removed samples were then filtered, washed with abundant methanol and vacuum dried overnight.

2.4 Synthesis of Ph-PMO

Brij 76 (0.5 g, 0.703 mmol) was dissolved in 2 M HCl (12.5 mL, 25.0 mmol) and distilled water (2.5 mL) in a round bottom flask with continuous magnetic stirring for 30 min at 50 °C. 1,4-Bis(triethoxysilyl) benzene (1.04 mL, 2.63 mmol) was then added to the mixture and the stirring was continued for another 20 h at 50 °C. The solid product was collected via filtration and was air-dried for 24 h. The surfactant template was removed by refluxing 1.0 g of dry solid with 150 ml of ethanol and conc. HCl (1.69 mL, 20.3 mmol) at 50 °C for 5 h. The surfactant removal step was repeated one more time. The final product was filtered, air-dried, and further dried under vacuum overnight.

2.5 Characterization

XRD patterns were recorded on a Bruker X–ray diffractometer using Cu Kα radiation (40 kV, 44 mA) over the range of 1–50 2θ degrees. Nitrogen sorption isotherms were measured on a Micromeritics Tristar surface area and porosity analyzer. The surface area and pore size distribution were calculated by the Brunauer Emmett Teller (BET) and Barrett Joyner Halenda (BJH) methods respectively. Elemental analyses of the dry samples were done by triplicate on a Perkin Elmer 2100 series II CHNS analyzer, using acetanilide as calibration standard and combustion and reduction temperatures of 925 °C and 640 °C respectively. Transmission Electron Microscopy (TEM) images were obtained using a FEI Tecnai G2 F20 scanning transmission electron microscope operating at 200 kV. TEM samples were prepared by placing 2-3 drops of dilute methanol suspensions onto a carbon-coated copper grid. Transmission mode FTIR measurements were made on a Bruker Vertex 80 FT-IR spectrometer equipped with a HeNe laser and photovoltaic MCT detector and OPUS software. Samples were mixed at ca. 2 wt% with KBr and pressed into pellets for analysis.

Relative polarity measurements of samples were done according to a previously published method.[36] A solution of Prodan in acetone (10 µL, 1.0 mM) was added to the samples (10.0 mg each), grinded, let dry, and suspended in water (2.0 mL). Fluorescence measurements of the suspensions were recorded in a Cary Eclipse Fluorescence Spectrophotometer. Excitation wavelength was set at 337 nm and both excitation and emission slit widths were set at 5 nm. Obtained fluorescence curves were fitted in origin pro using a Gaussian distribution model. Maximum fluorescence emission wavelength of

each sample was used to assign relative polarities based on probe fluorescence in reference solvents.[36]

2.6 Impregnation of Ibuprofen into mesoporous materials

Ibuprofen was introduced into the pores via incipient wetness impregnation. In brief, the mesoporous materials (30.0 mg each) were ground to a fine powder using a pestle in an agate mortar. A fresh solution of Ibuprofen in acetone (30 μL, 0.5 M) was then added dropwise to each material, and the mixture was ground until seemingly dry. The impregnated materials were then oven-dried to remove excess acetone, and then dried overnight under vacuum.

2.7 Preparation of simulated body fluid (SBF) solution.

This solution was prepared following the literature.[37] NaCl (7.996 g, 0.14 mmol), $NaHCO_3$ (0.350 g, 0.0042 mmol), KCl (0.224 g, 0.0030 mmol), K_2HPO_4 (0.174 g, 0.001 mmol), $MgCl_2 \cdot 6H_2O$ (0.305 g, 0.0015 mmol), 1M HCl (40.0 mL, 0.04 mmol), $CaCl_2$ (0.278 g, 0.0025 mmol), Na_2SO_4 (0.071 g, 0.0050 mmol), and tris(hydroxymethyl) aminomethane (6.057 g, 0.05 mmol) were dissolved in deionized water (500 mL) one by one in the above mentioned order in a 1L polyethylene bottle while stirring at 36.5 ºC. The pH of the solution was adjusted to 7.40 using a 1M HCl solution. The total volume of the solution was then adjusted to 1L by adding deionized water and shaking at 20 °C. The prepared SBF solution was stored in a refrigerator at 5 °C.

2.8 Ibuprofen release experiments

The Ibuprofen-loaded samples (30.0 mg each) were introduced into a dialysis membrane (Spectrum Labs, MW cutoff = 12-14 kDa) and immersed into SBF (10.0 mL). The intact SBF solution was continuously circulated through a quartz flow cuvette, and the absorption band at 263 nm was monitored for 20 h via UV-vis spectroscopy, taking scans every 5 min. Three separate release experiments were performed for each material, and the results were averaged.

2.9 Computational methods.

All calculations were performed using the dispersion-corrected B3LYP-D3[38] method implemented in the GAMESS[39] package using the 6-311G(d,p) basis set. Three different surfaces were optimized using the MCM-41 model developed by Ugliengo and collaborators.[34] The surfaces consisted of bare MCM-41 silica, and MCM-41 silica substituted with a phenyl group and with a phenethyl group. Ph-PMO was modeled based on previous work by Martinez and Pacchioni.[40] The structure corresponds to a sequence of six and four membered rings of organosilica tetrahedra with T3:T2 ratio of 2:1, based on the solid state NMR study by Comotti *et al*.[41] All of the models were optimized using the QM/MM SIMMOM[42] implemented in GAMESS, using the B3LYP-D3 functional with a 6-311(d,p) basis set.

3. Results and discussion

3.1 Material synthesis and characterization

To explore the effects of non-covalent interactions, group orientation and conformational flexibility on Ibuprofen release, MCM-41 type mesoporous silica nanoparticles (MSN) functionalized with phenyl (Ph-MSN) and phenethyl (PhEt-MSN) groups, and phenylene-bridged periodic mesoporous organosilica (Ph-PMO) were synthesized. Non-functionalized MSN was also prepared as a control (Scheme 1).

Characterization of the materials by nitrogen physisorption and x-ray diffraction revealed that the organic groups have no significant effects on the textural properties and pore geometry of the MSN samples. While all the MSN materials have similar surface areas (around 1200 m^2 g^{-1}), the surface of Ph-PMO is about 30% lower (807 m^2 g^{-1}) (Table 1, Fig. S1). However, the pore width distributions of all materials are very similar (centered at 2.6 – 3.0 nm), and all of them have 2D hexagonal arrays of pores as evidenced by XRD patterns and TEM images (Fig. S2, S3). While the loadings of phenyl groups are very similar for Ph-MSN and PhEt-MSN based on CHN elemental analysis, Ph-PMO has a much higher number of groups because its only precursor is the bis-siloxy-benzene.

The relative polarities of the pore surfaces were measured to determine if material hydrophobicity controls Ibuprofen release. Pore polarities were assessed via fluorescence spectroscopy of the impregnated molecular probe Prodan, as reported before (Table 1, Fig. 1, S4).[36] Because of the lack of organic moieties, the silanol-rich non-functionalized MSN has a much higher interfacial polarity than the other materials. Interestingly, Ph-MSN has a higher polarity than PhEt-MSN, likely due to the differences

in flexibility of the two surface groups. While the rigid Ph groups in Ph-MSN expose the surface silanols allowing their contribution to the interfacial polarity, the flexible PhEt can bend over the surface and mask some of the polar silanols to decrease their contribution.[43] Interestingly, in spite of the larger amount of phenyl groups in Ph-PMO, its relative polarity is very similar to that of PhEt-MSN. This result supports the idea that the phenyl groups in PhEt-MSN may lay flat on the surface covering a fraction of silanols thus giving a balance of hydrophobic-hydrophilic groups comparable to that of Ph-PMO.

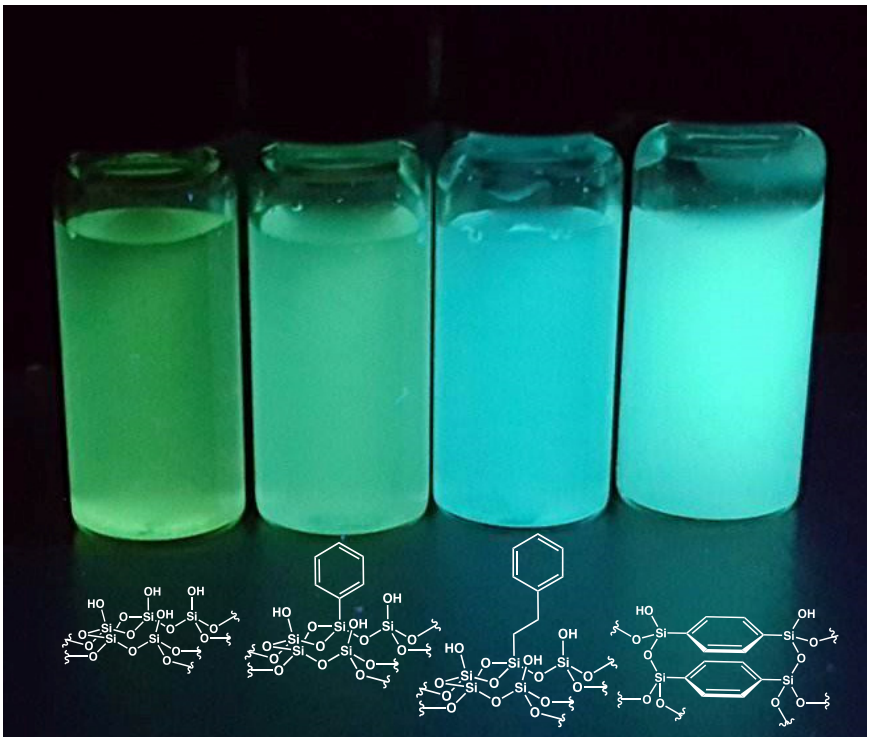

Fig. 1. Photograph of aqueous suspensions of (left to right) MSN, Ph-MSN, PhEt-MSN, and Ph-PMO loaded with the solvatochromic fluorophore Prodan. Interfacial polarity is proportional to the wavelength of emission (i.e. green and blue indicate high and low polarity respectively).[36]

FTIR analysis of the materials (Fig. S5) evidenced features common to all of them, including the characteristic intense peaks centered at ca. 1090 cm^{-1} and 3400 cm^{-1} assigned to Si–O–Si and –O–H stretching vibrations respectively, the latter corresponding to H-bonding silanols and physisorbed water. Presence of water in all the materials is confirmed by a clear signal of the scissor bending vibration at 1630 cm^{-1}. The organic groups are characterized in Ph-MSN, PhEt-MSN and Ph-PMO by peaks in the 3000 – 3100 cm^{-1} region corresponding to aromatic C–H stretching vibrations, and 1380 – 1420 cm^{-1} region attributed to aromatic ring vibrations and Si–C stretching. These signals are much better defined in Ph-PMO due to the larger number of organic groups in the material. Additional absorption between 2900 and 3000 cm^{-1} is visible for PhEt-MSN corresponding to the aliphatic C–H bonds of the ethylene groups.

Table 1. Physicochemical properties of the materials.

	S_{BET} (m^2 g^{-1})	W_{BJH} (nm)	Relative polarity[a]	Phenyl groups (mmol g^{-1})[b]
MSN	1262	3.0	1.00 ± 0.01	--
Ph-MSN	1221	2.6	0.84 ± 0.02	1.2
PhEt-MSN	1196	2.6	0.69 ± 0.01	1.0
Ph-PMO	807	2.8	0.72 ± 0.01	3.2[c]

[a]Determined by fluorescence measurement of solvatochromic probe Prodan.[36]

[b]Determined by CHN elemental analysis. [c]Estimated from the surface area of the material and its structural model.[44]

3.2 Ibuprofen loading

Ibuprofen was loaded into the materials via incipient wetness impregnation to facilitate drug penetration into the pores by capillary action.[45] The amount loaded (0.5

mmol g^{-1}) was selected to ensure there were plenty of phenyl groups in the materials to interact with the drug. Drug loading is confirmed by FTIR analysis of the impregnated materials which show a clear absorption band at 1710 cm^{-1} corresponding to the C=O stretching of Ibuprofen (Fig. 2). This signal is red-shifted by ca. 14 cm^{-1} in all of the loaded materials with respect to the pure drug suggesting interaction of the group with the surface, likely via hydrogen bonding with silanol groups.[26] Smaller blue shifts in ring vibration bands (1462 to 1467 cm^{-1} and 1508 to 1514 cm^{-1}) suggest that the aromatic group is either interacting with the surface or its mobility is significantly restricted likely due to confinement in the porous materials.[46-48] Wide angle XRD analysis of the drug-loaded materials does not show crystalline Ibuprofen reflections in any of the materials (Fig. S6), which is consistent with previous reports and has also been attributed to confinement of the drug into the pores.[26]

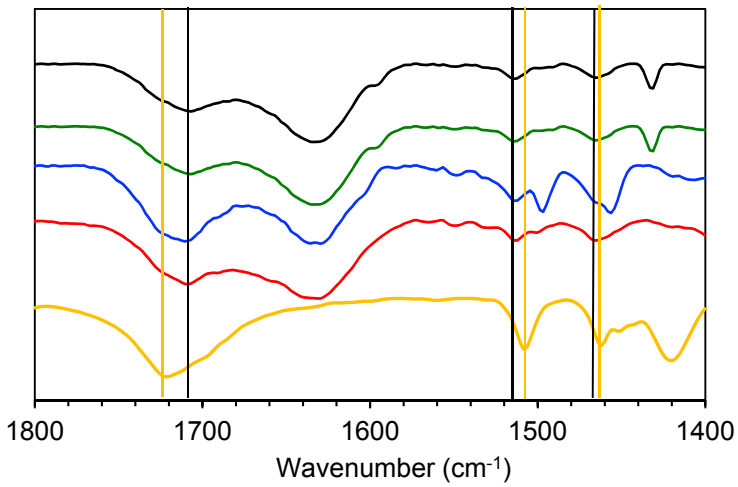

Fig. 2. FTIR spectra of Ibuprofen-loaded MSN (black), Ph-MSN (green), PhEt-MSN (blue) and Ph-PMO (red). Spectrum of the free drug (KBr pellet) is in yellow.

3.3 Ibuprofen release from different MSN

The release of Ibuprofen from the materials to simulated body fluid (SBF) was monitored via UV-visible spectroscopy (λ = 263 nm). The drug-loaded materials were set in a dialysis bag (MW cutoff = 12–14 kDa) and immersed in SBF (Fig. S7). The solution was continuously circulated through a quartz flow cuvette and spectra were acquired every 5 min for 20 h.

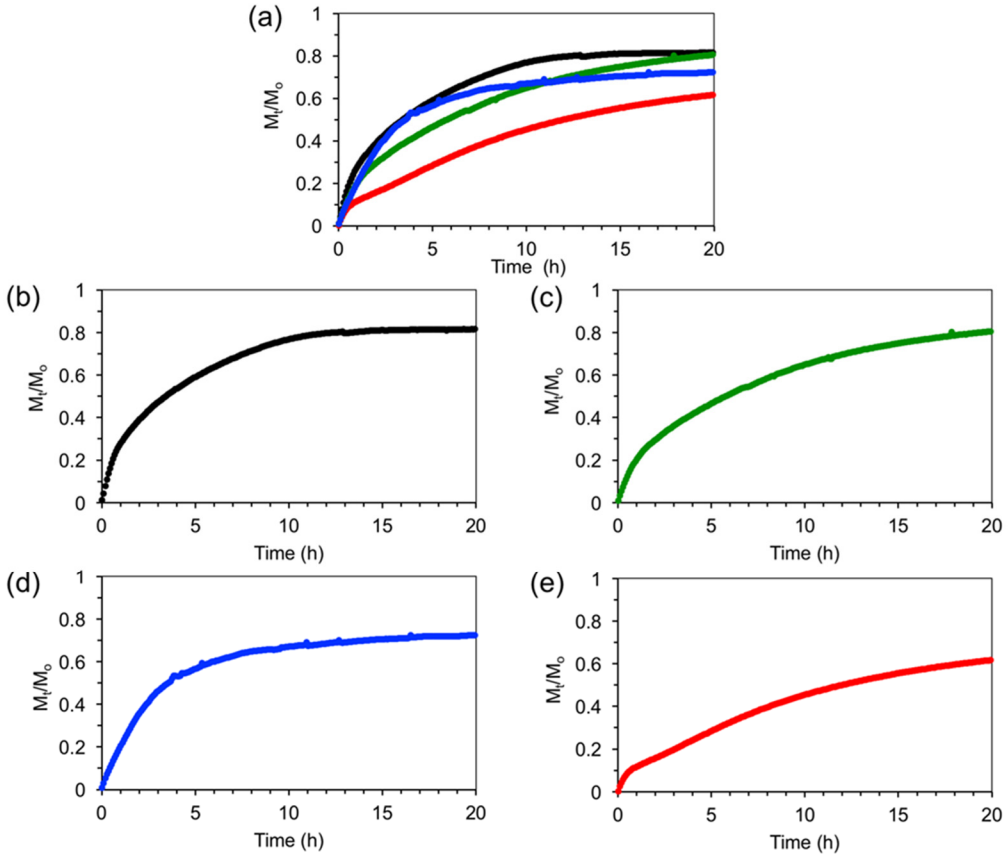

Fig. 3. Average release profiles of Ibuprofen from the DDS. M_t/M_o is the fraction of Ibuprofen released at a given time t. (a) Overlaid profiles of all materials. (b-e) Individual profiles: (b) MSN (black), (c) Ph-MSN (green), (d) PhEt-MSN (blue), (e) Ph-PMO (red). The colors in (a) correspond to those in (b-e).

The average Ibuprofen release profiles indicate a clear dependence on the functionality of the silica materials (Fig. 3, Table 2). Some of the most relevant differences between the profiles include: 1) only MSN and PhEt-MSN reach a plateau within the experimental timeframe (less than 1% change after 12 and 16 h, respectively), 2) MSN and Ph-MSN show the largest cumulative release after 20 h (ca. 82 ± 3% and 81 ± 4%, respectively), 3) MSN presents a higher initial release rate than the other materials, all of which present the same values (0.44 versus 0.25 mM h^{-1} respectively), 4) while all the phenyl-bearing materials give the same initial rates, PhEt-MSN sustains it for a longer time (2 h) than Ph-MSN (1.5 h) and Ph-PMO (0.5 h). These differences indicate that the phenyl groups indeed have an effect on the adsorption and retention of Ibuprofen, and are consistent with the phenyl-bearing materials having lower polarity (i.e. more hydrophobicity) than the non-functionalized MSN. However, the differences observed between the drug release profiles of all the phenyl-functionalized materials cannot be explained by hydrophobicity alone. The different release profiles from these materials must be due to significant variations in the drug-surface interactions at the molecular level, which are likely regulated by the relative orientation and flexibility of binding sites on the surface.

Table 2. Descriptors of Ibuprofen release from the mesoporous materials.

Material	20 h release (%)	Initial rate (mM h^{-1})	Initial rate regime (h)
MSN	82 ± 3	0.44	0.8
Ph-MSN	81 ± 4	0.25	1.5
PhEt-MSN	73 ± 2	0.25	2.0
Ph-PMO	62 ± 4	0.25	0.5

3.4 Kinetic and thermodynamic analysis of Ibuprofen release

To better understand the differences between the materials the drug release data were fitted to a kinetic model developed by Wu and co-workers.[49] The model deconvolutes the contributions of pore diffusion and drug-support interactions from the release profiles, and is defined by three fundamental parameters: the diffusion/convection rate constant (k_s), and the rate constants for adsorption (k_{on}) and desorption (k_{off}) of the drug from the support. The experimental release profiles are fitted to the model equation:

$$\frac{M_t}{M_0} = \frac{k_{off}}{k_{on}+k_{off}}(1 - e^{-k_s t}) + \frac{k_{on}}{k_{on}+k_{off}}(1 - e^{-k_{off} t}) \qquad (1)$$

where M_t and M_0 are the cumulative drug release at time t and the initial drug amount, respectively, and the kinetic constants k_s, k_{on}, and k_{off} are defined as above. In addition, the partition equilibrium between the surface and the solvent is defined by the ratio k_{on}/k_{off}, and the associated free energy change that controls the burst-release phase is related to this ratio by:

$$\Delta G = -k_B\, T\, ln(\frac{k_{on}}{k_{off}}) \qquad (2)$$

where k_B is the Boltzmann constant and T the absolute temperature. Fitting of the average release profiles to equation (1) gives high correlation coefficients ($R^2 > 0.98$ for each profile, Fig. S8), and provides kinetic constants for Ibuprofen release from each material (Table 3).

Table 3. Kinetic and thermodynamic parameters for the release of Ibuprofen from all of the materials.

	k_s (h^{-1})	k_{on} (h^{-1})	k_{off} (h^{-1})	$\Delta G \times 10^{21}$ (J)
MSN	0.377 ± 0.012	0.019 ± 0.003	0.037 ± 0.003	2.80 ± 1.44
Ph-MSN	0.836 ± 0.031	0.227 ± 0.007	0.074 ± 0.0005	-4.63 ± 0.04
PhEt-MSN	0.376 ± 0.003	0.005 ± 0.0004	0.010 ± 0.0006	2.71 ± 0.72
Ph-PMO	0.242 ± 0.019	0.104 ± 0.016	0.035 ± 0.001	-4.47 ± 0.22

It is clear from the release profiles and the fitted curves that none of the materials will achieve 100% release. This behavior clearly indicates the systems tend to reach a partition equilibrium, ultimately regulated by the relative strengths of the surface-drug and solvent-drug interactions as well as the entropy of the system. This equilibrium is described by the sign and magnitude of ΔG. The sign of ΔG is indicative of the strength of interaction between the surface and the drug. The positive ΔG for MSN and PhEt-MSN indicates that desorption of the drug from the surface is favored ($k_{off} > k_{on}$) leading to the burst type release observed in Fig. 3b,d. To the contrary, ΔG for Ph-MSN and Ph-PMO is negative, indicating strong interactions with the drug that hinder desorption ($k_{off} < k_{on}$), and is reflected by a more sustained type of release (Fig. 3c,e). While ΔG of Ibuprofen with Ph-MSN indicates a strong adsorption, its cumulative release after 20 h is the same as MSN and higher than PhEt-MSN, both of which have weaker interactions with the drug. The magnitude of the cumulative release is proportional to the rate of diffusion from the pores to the SBF media (k_s), which is also higher for Ph-MSN than for MSN and PhEt-MSN. This apparent contradiction between the difference in strength of interaction and the diffusion kinetics and cumulative drug release from these materials is explained by examining the magnitudes of k_{on} and k_{off}. While the ratio of these two

parameters favors adsorption for Ph-MSN, both k_{on} and k_{off} are significantly higher indicating that the drug exchanges quickly between adsorbed and desorbed state in this material, which leads to a higher probability of reaching the end of the pores and escape to the surrounding SBF solution. This also explains why PhEt-MSN, despite having the same k_s and ΔG as MSN, gives a lower cumulative 20 h release: the much lower adsorption and desorption rate constants decrease the probabilities of the drug reaching the end of the pores for discharge into SBF.

3.5 Computational modeling of Ibuprofen-surface interactions

DFT calculations were performed to understand the differences between the interaction of Ibuprofen with the mesoporous materials. For the functionalized MSNs, the models used were based on a silica slab reported by Ugliengo and collaborators.[34, 35] The different surfaces were modified with the respective organic groups and optimized using the hybrid QM/MM SIMOMM method.[42] The Ph-PMO structure was produced based on the model developed by Martinez and Pacchioni.[40]

The possible interactions of Ibuprofen with the materials' surfaces are H-bonding between –COOH and silanol groups, and π-π interactions between the phenyl rings in the drug and the rings on the surface. The optimized structures showed a significant difference in the O-H distances corresponding to H-bonds between the non-functionalized MSN (1.97 Å) and phenyl-bearing materials (Ph-MSN 1.76 Å and PhEt 1.72Å) (Fig. 4, S9). This suggests a weaker interaction of the former with the surface, a result that is consistent with the highest experimental rate and extent of release observed for MSN.

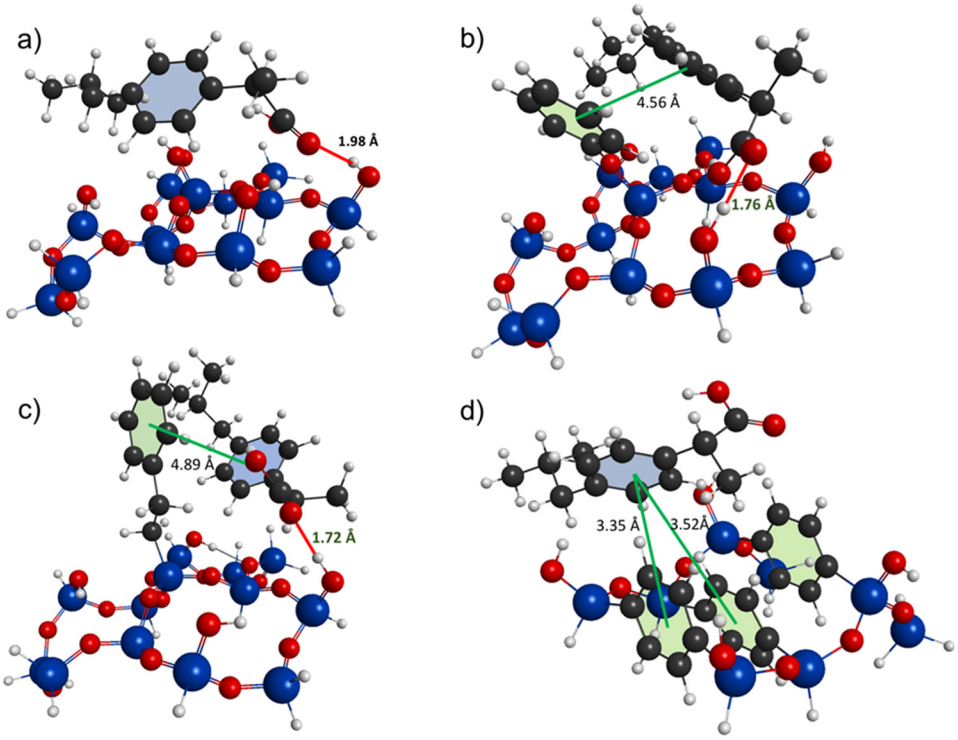

Fig. 4. QM section of the optimized structures of Ibuprofen interacting with (a) MSN, (b) Ph-MSN, (c) PhEt-MSN, and (d) Ph-PMO. For clarity, the surface phenyl rings are shaded green and the Ibuprofen phenyl rings are shaded blue.

While the slightly shorter O-H distance in PhEt-MSN than Ph-MSN would suggest a stronger interaction of the drug with the former, the ΔG of adsorption derived from their release profiles indicate the opposite behavior. However, as pointed out by Ugliengo *et al.*, H-bonding is not the dominant interaction between Ibuprofen and a silica surface.[24] Thus, it is likely that the experimental differences observed between the release profiles of Ibuprofen from these two materials are due to π-π interactions between the aromatic rings. Further analysis of the optimized complexes reveals differences in the relative positions of the phenyl groups in the drug with respect to the surface phenyl groups (Fig. S10). While there are clear deviations from ideal stacking in all of the

interacting pairs, the misalignment with the ring in Ibuprofen is larger in PhEt-MSN: the average distances between aromatic carbons of the rings are longer (4.89 Å versus 4.56 Å) and the diverging angle is wider (39° versus 28°) than in Ph-MSN (Fig. S10). These differences in interaction geometries are likely the main reason for the more favorable ΔG of adsorption of the drug with Ph-MSN, and for the observed differences in drug release profiles between the materials.

Analysis of Ph-PMO indicates much shorter distances between its phenyl rings and those of the drug (3.35 and 3.52 Å). In addition, while the π-π interactions of Ibuprofen with Ph-MSN and PhEt-MSN tend to be face-to-face, the relative orientation of the rings in the drug-Ph-PMO model indicates the interaction is edge-to-face. Because of the quadrupolar nature of phenyl rings, edge-to-face interactions are generally stronger than face-to-face.[50] These results suggest that the interaction of the drug with Ph-PMO must be stronger than with Ph-MSN and PhEt-MSN, and are in agreement with the negative ΔG and lowest rate and extent of Ibuprofen release observed for this material. Additional experiments aimed at identifying the geometry of the specific surface-Ibuprofen interactions and the mobility of the adsorbed drug via solid-state NMR,[51,52] as well as the quantitative relationship between phenyl group density and Ibuprofen release profiles are currently in progress in our laboratories.

Conclusions

In summary, the kinetics and cumulative release of Ibuprofen from mesoporous silica DDS can be controlled by modification of the carrier's surface with phenyl groups. The presence of phenyl groups on the surface decreases the initial rate of release, in

principle due to a decrease in interfacial polarity that affects the partition equilibrium between the surface and the aqueous SBF. Controlling the orientation and conformational flexibility of the surface phenyl groups uncovers subtle differences in intermolecular interactions that allow further fine-tuning the drug release profiles. At the molecular level, incorporation of phenyl groups on silica surfaces results in stronger drug-surface interactions arising from cooperativity between COOH-silanol H-bonding and π-π interactions with the surface phenyl groups. The negative ΔG of Ph-MSN and positive ΔG of PhEt-MSN suggest that π-π interactions contribute more to Ibuprofen adsorption than H-bonding, because the former has closer and better phenyl ring alignment but longer O-H distances than the latter. While these two systems possess silanols and phenyl rings, it appears that the locked conformation of phenyl groups in Ph-MSN provides a better fit for Ibuprofen docking than the phenyl groups with mobile ethylene linkers in PhEt-MSN. This conformational rigidity of Ph-MSN appears to facilitate a rapid drug adsorption/desorption equilibrium evidenced by the large k_{on} and k_{off} values that eventually lead to a high cumulative release after long contact times. In contrast to Ph-MSN and PhEt-MSN where the phenyl rings of Ibuprofen tend to interact face-to-face, the π-π interaction of the drug with Ph-PMO seems to be edge-to-face. This type of interaction in Ph-PMO is stronger than the face-to-face and explains the slower kinetics and cumulative release of Ibuprofen observed for this material. These results demonstrate that careful selection and design of drug-surface interactions can be a valuable tool to precisely tune the sustained release of drugs for custom therapeutic applications.

Acknowledgements

This research is supported by the U.S. Department of Energy, Office of Basic Energy Sciences, Division of Chemical Sciences, Geosciences, and Biosciences, through the Ames Laboratory Catalysis Science program. The Ames Laboratory is operated for the U.S. Department of Energy by Iowa State University under Contract No. DE-AC02-07CH11358.

References.

[1] I.I. Slowing, J.L. Vivero-Escoto, B.G. Trewyn, V.S.-Y. Lin, J. Mater. Chem., 20 (2010) 7924 - 7937.
[2] E. Aznar, M. Oroval, L. Pascual, J.R. Murguía, R. Martínez-Máñez, F. Sancenón, Chem. Rev., 116 (2016) 561-718.
[3] D. Tarn, C.E. Ashley, M. Xue, E.C. Carnes, J.I. Zink, C.J. Brinker, Acc. Chem. Res., 46 (2013) 792-801.
[4] I.I. Slowing, J.L. Vivero-Escoto, C.-W. Wu, V.S.Y. Lin, Adv. Drug Deliv. Rev., 60 (2008) 1278-1288.
[5] M. Vallet-Regí, F. Balas, D. Arcos, Angew. Chem., Int. Ed., 46 (2007) 7548-7558.
[6] C. Argyo, V. Weiss, C. Bräuchle, T. Bein, Chem. Mater., 26 (2013) 435-451.
[7] W. Gao, J.M. Chan, O.C. Farokhzad, Mol. Pharm., 7 (2010) 1913-1920.
[8] A. Tukappa, A. Ultimo, C. de la Torre, T. Pardo, F. Sancenón, R. Martínez-Máñez, Langmuir, 32 (2016) 8507-8515.
[9] Y. Zhao, B.G. Trewyn, I.I. Slowing, V.S.Y. Lin, J. Am. Chem. Soc., 131 (2009) 8398-+.
[10] R. Mortera, J. Vivero-Escoto, Slowing, II, E. Garrone, B. Onida, V.S.Y. Lin, Chem. Commun., (2009) 3219-3221.
[11] J.L. Vivero-Escoto, I.I. Slowing, C.-W. Wu, V.S.-Y. Lin, J. Am. Chem. Soc., 131 (2009) 3462-3463.
[12] F.M. Martín-Saavedra, E. Ruíz-Hernández, A. Boré, D. Arcos, M. Vallet-Regí, N. Vilaboa, Acta Biomater., 6 (2010) 4522-4531.
[13] J.L. Vivero-Escoto, Slowing, II, V.S.Y. Lin, Biomater., 31 (2010) 1325-1333.
[14] I.I. Slowing, J.L. Vivero-Escoto, Y. Zhao, K. Kandel, C. Peeraphatdit, B.G. Trewyn, V.S.Y. Lin, Small, 7 (2011) 1526-1532.
[15] I. Slowing, B.G. Trewyn, V.S.Y. Lin, J. Am. Chem. Soc., 128 (2006) 14792-14793.
[16] L. Pan, Q. He, J. Liu, Y. Chen, M. Ma, L. Zhang, J. Shi, J. Am. Chem. Soc., 134 (2012) 5722-5725.
[17] C.-P. Tsai, C.-Y. Chen, Y. Hung, F.-H. Chang, C.-Y. Mou, J. Mater. Chem., 19 (2009) 5737-5743.
[18] J. Tu, T. Wang, W. Shi, G. Wu, X. Tian, Y. Wang, D. Ge, L. Ren, Biomater., 33 (2012) 7903-7914.
[19] J. Lu, M. Liong, Z. Li, J.I. Zink, F. Tamanoi, Small, 6 (2010) 1794-1805.

[20] F. Chen, H. Hong, Y. Zhang, H.F. Valdovinos, S. Shi, G.S. Kwon, C.P. Theuer, T.E. Barnhart, W. Cai, ACS Nano, 7 (2013) 9027-9039.
[21] J.E. Lee, N. Lee, T. Kim, J. Kim, T. Hyeon, Acc. Chem. Res., 44 (2011) 893-902.
[22] J.C. Doadrio, E.M.B. Sousa, I. Izquierdo-Barba, A.L. Doadrio, J. Perez-Pariente, M. Vallet-Regi, J. Mater. Chem., 16 (2006) 462-466.
[23] R.-A. Mitran, C. Matei, D. Berger, J. Phys. Chem. C, 120 (2016) 29202-29209.
[24] M. Delle Piane, M. Corno, A. Pedone, R. Dovesi, P. Ugliengo, J. Phys. Chem. C, 118 (2014) 26737-26749.
[25] M. Delle Piane, S. Vaccari, M. Corno, P. Ugliengo, J. Phys. Chem. A, 118 (2014) 5801-5807.
[26] T. Azaïs, C. Tourné-Péteilh, F. Aussenac, N. Baccile, C. Coelho, J.-M. Devoisselle, F. Babonneau, Chem. Mater., 18 (2006) 6382-6390.
[27] F. Babonneau, L. Yeung, N. Steunou, C. Gervais, A. Ramila, M. Vallet-Regi, J. Sol-Gel Sci. Technol., 31 (2004) 219-223.
[28] A.R. Brás, E.G. Merino, P.D. Neves, I.M. Fonseca, M. Dionísio, A. Schönhals, N.T. Correia, J. Phys. Chem. C, 115 (2011) 4616-4623.
[29] F. Guenneau, K. Panesar, A. Nossov, M.-A. Springuel-Huet, T. Azais, F. Babonneau, C. Tourne-Peteilh, J.-M. Devoisselle, A. Gedeon, Phys. Chem. Chem. Phys., 15 (2013) 18805-18808.
[30] A.R. Brás, J.P. Noronha, A.M.M. Antunes, M.M. Cardoso, A. Schönhals, F. Affouard, M. Dionísio, N.T. Correia, J. Phys. Chem. B, 112 (2008) 11087-11099.
[31] A.R. Brás, I.M. Fonseca, M. Dionísio, A. Schönhals, F. Affouard, N.T. Correia, J. Phys. Chem. C, 118 (2014) 13857-13868.
[32] L. Zeng, L. An, X. Wu, J. Drug Deliv., 2011 (2011) 370308.
[33] L. Zeng, X. Wu, Appl. Phys. Lett., 97 (2010) 073701.
[34] P. Ugliengo, M. Sodupe, F. Musso, I.J. Bush, R. Orlando, R. Dovesi, Adv. Mater., 20 (2008) 4579-4583.
[35] B. Coasne, P. Ugliengo, Langmuir, 28 (2012) 11131-11141.
[36] D. Singappuli-Arachchige, J.S. Manzano, L.M. Sherman, I.I. Slowing, ChemPhysChem, 17 (2016) 2982-2986.
[37] T. Kokubo, H. Kushitani, S. Sakka, T. Kitsugi, T. Yamamuro, J. Biomed. Mater. Res., 24 (1990) 721-734.
[38] S. Grimme, J. Antony, S. Ehrlich, H. Krieg, J. Chem. Phys., 132 (2010) 154104.
[39] M.W. Schmidt, K.K. Baldridge, J.A. Boatz, S.T. Elbert, M.S. Gordon, J.H. Jensen, S. Koseki, N. Matsunaga, K.A. Nguyen, S. Su, T.L. Windus, M. Dupuis, J.A. Montgomery, J. Comp. Chem., 14 (1993) 1347-1363.
[40] U. Martinez, G. Pacchioni, Microporous Mesoporous Mater., 129 (2010) 62-67.
[41] A. Comotti, S. Bracco, P. Valsesia, L. Ferretti, P. Sozzani, J. Am. Chem. Soc., 129 (2007) 8566-8576.
[42] J.R. Shoemaker, M.S. Gordon, J. Phys. Chem. A, 103 (1999) 3245-3251.
[43] K. Mao, T. Kobayashi, J.W. Wiench, H.-T. Chen, C.-H. Tsai, V.S.Y. Lin, M. Pruski, J. Am. Chem. Soc., 132 (2010) 12452-12457.
[44] S. Inagaki, S. Guan, T. Ohsuna, O. Terasaki, Nature, 416 (2002) 304-307.
[45] X. Zhu, H.-r. Cho, M. Pasupong, J.R. Regalbuto, ACS Catal., 3 (2013) 625-630.
[46] A. Jubert, M.L. Legarto, N.E. Massa, L.L. Tévez, N.B. Okulik, J. Mol. Struct., 783 (2006) 34-51.

[47] C.R. Gordijo, C.A.S. Barbosa, A.M. Da Costa Ferreira, V.R.L. Constantino, D.d. Oliveira Silva, J. Pharm. Sci., 94 (2005) 1135-1148.
[48] M.V. Kandziolka, M.K. Kidder, L. Gill, Z. Wu, A. Savara, Phys. Chem. Chem. Phys., 16 (2014) 24188-24193.
[49] L. Zeng, L. An, X. Wu, J. Drug Deliv., 2011 (2011) 15.
[50] M.O. Sinnokrot, E.F. Valeev, C.D. Sherrill, J. Am. Chem. Soc., 124 (2002) 10887-10893.
[51] Y. Shi, M. van Steenbergen, E.A. Teunissen, L. Novo, S. Gradmann, M. Baldus, C.F. van Nostrum, W.E. Hennink, Biomacromol., 14 (2013) 1826-1837.
[52] S. Nedd, T. Kobayashi, C.H. Tsai, I.I. Slowing, M. Pruski, M.S. Gordon, J. Phys. Chem. C, 115 (2011) 16333-16339.

Graphical abstract